ACS Sustainable Chemistry & Engineering

pubs.acs.org/journal/ascecg

Research Article

Marine Toxicity, Biodegradability, and Rolling-Sliding Tribological Performance of Ionic Liquid-Enhanced Environmentally-Acceptable Lubricants for Tidal Turbomachinery

Wenbo Wang, Peijia Ku, Louise M. Stevenson, Chanaka Kumara, Harry M. Meyer, III, Huimin Luo, Teresa J. Mathews, and Jun Qu*

Cite This: *ACS Sustainable Chem. Eng.* 2025, 13, 12482−12495

Read Online

ACCESS | Metrics & More | Article Recommendations | Supporting Information

ABSTRACT: Environmentally acceptable lubricants (EALs) are increasingly being recognized in many fields including waterpower, hydraulics, water transport, agricultural machinery, offshore wind turbines, etc. Specifically, high-performance EALs are demanded for tidal turbomachinery to ensure high efficiency and reliability and avoid the significant risk of direct contamination of the marine ecosystem upon leaks. Here we report a new development of ionic liquid (IL)-enhanced EALs for tidal energy. One short-chain phosphonium phosphate and one short-chain ammonium phosphate ILs were used as the candidate additives and the IL-containing EALs demonstrated significantly improved lubricating performance, much lower toxicity, and increased biodegradability compared with commercial baselines. Specifically, in a rolling-sliding test simulating the operation of a model tidal turbine gearbox bearing, an EAL containing the ILs at a 0.5 wt % concentration demonstrated 40% lower friction, 45% less wear loss, substantially reduced rolling contact fatigue-induced surface damage, and one order of magnitude lower vibration noise compared with a commercial gear oil. In an EPA standard toxicity test, 90 and 70% survival of marine biota was observed when exposed to an EAL containing 5 wt % of the short-chain phosphonium phosphate and ammonium phosphate ILs, respectively, while the selected commercial gear oil and bioderived additive killed all marine biota. In a standard biodegradability test, 2 wt % addition of the phosphonium phosphate IL not only retained the EAL's ready biodegradability but further boosted the oil decomposition from a range of 60−80% to a higher level of 80−95%. Conversely, adding the commercial bioderived additive downgraded the EAL from readily to inherently biodegradable. This work offers scientific insights for development of ILs as potential EAL additives for marine energy and broader applications.

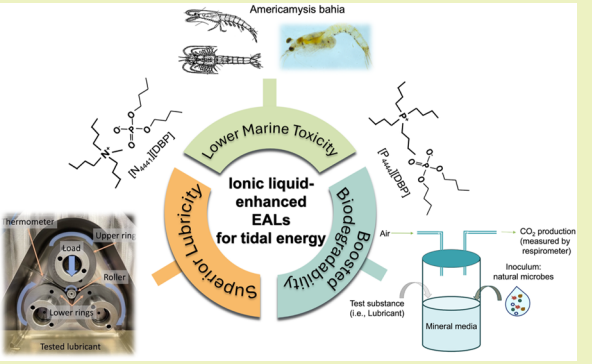

KEYWORDS: *environmentally acceptable lubricants (EALs), additives, ionic liquids, marine toxicity, biodegradability*

1. INTRODUCTION

Tidal energy, a type of power generated by the gravitational interaction between the Earth, Sun, and Moon, is attracting considerable interest due to its stability, predictability, and efficiency without greenhouse gas emissions.[1,2] The technical power potential of U.S. tidal energy resources is estimated to be 220 TWh/yr, which is more than 5% of U.S. annual electricity generation.[3] Because >50% of the U.S. population lives within 50 miles of the coast, tidal energy can power electric microgrids in densely populated or remote coastal areas enhancing energy and coastal resilience. Further, tidal energy can generate electricity around the clock and is less dependent on the climate than wind energy. The relatively higher density of seawater (~832 times greater than air) enables a tidal turbine to extract a 61% higher maximum power for an equivalent input power compared with a wind turbine.[4] To date, there are three common technologies for extracting the tidal energy, namely, tidal barriers, tidal lagoons, and tidal streams. They utilize the kinetic or potential energy from the tidal flow through tidal turbines to move the blades connected to an electrical power generator, e.g., horizontal-axis tidal turbines and vertical-axis tidal turbines in tidal streams.[5]

Tidal turbines need to endure the harsh underwater environment with a high degree of reliability because they are placed in a subsea environment and thus are difficult and expensive to repair and service once deployed. Although tidal turbines share similar drivetrain designs with wind turbines, they

Received: April 11, 2025
Revised: July 22, 2025
Accepted: July 23, 2025
Published: July 30, 2025

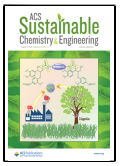

often operate at higher torques and lower speeds as a result of the higher density and resistance of water compared with air.[4] A tidal turbine operates at very slow rotor speeds of 7−20 rpm[6] and, as a result, the gear and bearing interfaces inevitably fall into boundary lubrication,[7] i.e., interface not fully separated by an oil film and involving metal−metal contact. The gearbox is expected to experience the longest downtime per failure among all tidal turbine drivetrain components.[8] About 70% of gearbox failures are due to wear and rolling contact fatigue (RCF) of the bearings.[9,10] Specifically, the low-speed front bearings endure cyclic radial loads and the high-speed rear bearings carry both radial and thrust loads.[11]

Besides the drivetrain design and materials selection, the gear oil plays a critical role in protecting the bearings and gears from wear and RCF.[12] Most current tidal turbine lubricants are borrowed from wind turbines. Synthetic oils, such as polyalkylene glycol (PAG) and polyalphaolefin (PAO), are preferred for wind and tidal turbines due to their higher thermal stability or slower aging allowing longer service intervals. Apart from the base oil, lubricant additives, e.g., antioxidant, antiwear (AW), extreme pressure (EP), antifoam, anticorrosion and etc., are also crucial.[13] Wear is inevitable in boundary lubrication that the tidal turbine gearbox experiences and surface protection largely relies on the AW and/or EP additives to chemically react with the contact surfaces to in situ form an protective solid tribofilm.

Another requirement for tidal turbine lubrication is environmental acceptance. Most commercial gear oils are toxic and/or not biodegradable and thus pose a serious threat to the marine ecosystems through inevitable leaks or spills.[14,15] Criteria for Environmentally Acceptable Lubricants (EALs) have been established by the U.S. Environmental Protection Agency (EPA).[16] Multiple groups of EAL base oils are available including water, vegetable oil, synthetic ester, and polyalkylene glycol (PAG).[13] However, lubricant additives that are both environmentally friendly and effective in protecting against wear are lacking.[17] Conventional AWs/EPs often contain heavy metal, halogen, and/or sulfur compounds[18] and thus cannot meet the environmental requirements, e.g., toxicity and biodegradability. Vegetable oils (VOs),[15] e.g., garlic oil,[19] soybean oil,[20] and sunflower oil,[21] have been studied as EAL additives, but their relatively low thermal and oxidative stability as well as poor cryogenic fluidity remain problematic. Carbon-based lubricant additives[22] such as nanodiamonds, carbon nanotubes and graphite have also gained interest as potential EAL additives,[23] but their oil dispersion and competing surface adsorption with other additives are of concern.[24] In addition, the toxicity of carbon-based additives for human health and their environmental impact remain controversial.[25,26]

Since the solubility problem of ionic liquids (ILs) in nonpolar oils was solved in 2012,[27,28] ILs have been extensively studied as lubricant additives owing to their unique physicochemical properties and molecular design flexibility.[29] Especially, ILs have demonstrated to be effective in reducing sliding wear and friction[30,31] and mitigating RCF[32] through strong surface adsorption and self-healing tribofilm formation by tribochemical reactions.[33] While a few literature studies[34−36] had claimed ILs as EALs, they did not provide any direct supporting evidence on the ILs' toxicity or biodegradability. In fact, our recent aquatic chronic toxicity tests found that the ILs previously developed for automotive lubrication were nearly as toxic as conventional oil additives.[37] In broader ILs research, toxicity and biodegradability measurements have been conducted on certain groups of ILs, but those ILs have not been proven to be suitable for lubrication.

We recently invented a new class of eco-friendly, high-lubricity ILs with short alkyl chains at Oak Ridge National Laboratory (ORNL).[38] Phosphonium phosphate and ammonium phosphate ILs containing alkyls of four carbons or less were identified as promising candidates for balancing the oil solubility, thermal stability, toxicity, and lubricity.[37] These new ILs not only performed well as EAL additives in a sliding contact with effective friction and wear reductions, but also exhibited significantly lower toxicity than commercial AW and EP additives and previous ILs in EPA standard fresh water toxicity tests, as reported in our previous work.[37,39]

The present study investigated the feasibility of the newly invented eco-friendly ILs as candidate EAL additives for lubricating a rolling-sliding bearing contact, with a target application for the gearbox in a tidal turbine. The marine toxicity, biodegradability, and tribological results of selected EAL base oils additized by the eco-friendly ILs were benchmarked against those of a commercial gear oil and the same EAL base oils containing a commercial bioderived additive at the same concentration. It should be noted that this study assessed the overall toxicity, biodegradability, and lubricating performance of the IL-additized lubricants rather than neat ILs. Results from this study provide a scientific basis for development of IL-additized EALs for tidal turbine and broader applications.

2. EXPERIMENTAL METHODS

2.1. Ionic Liquids. Two candidate ILs, $[P_{4444}][DBP]$ and $[N_{4441}][DBP]$, as shown in Figure 1, were selected based on our earlier fundamental work[37,39] and synthesized at ORNL's organic chemistry laboratory. The detailed synthesis process was described in.[37,39]

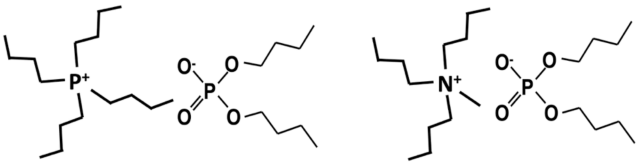

$[P_{4444}][DBP]$ $[N_{4441}][DBP]$

Figure 1. Molecular structures of $[P_{4444}][DBP]$ (left) and $[N_{4441}][DBP]$ (right).

The ^1H nuclear magnetic resonance (NMR) spectra of these two ILs were measured with a Bruker MSL-400 at 400 MHz. Spectrum was obtained in $CDCl_3$ with reference to TMS (0 ppm) for ^1H for $[N_{4441}][DBP]$ and using DMSO-d_6, as solvent for $[P_{4444}][DBP]$, as summarized in Table S1 in the Supporting Information. Their infrared spectra were recorded with Fourier transform infrared (FTIR) spectrometer (PerkinElmer Frontier FTIR) as presented in Figure S1 in the Supporting Information. The ^1H NMR spectrum of $[N_{4441}][DBP]$ has typical peaks of $N-CH_2$, $N-CH_2CH_2$, $N-CH_2CH_2CH_2$, and $N-CH_2CH_2CH_2CH_3$, and that of $[P_{4444}][DBP]$ contains $P-CH_2$, $P-CH_2CH_2$, $P-CH_2CH_2CH_2$, and $P-CH_2CH_2CH_2CH_3$. Both ILs showed peaks of $P-O-(CH_2)$, $P-O-(CH_2CH_2)$, $P-O-(CH_2CH_2CH_2)$, and $P-O-(CH_2CH_2CH_2\ CH_3)$. The FTIR spectrum of $[N_{4441}][DBP]$ shows strong peaks of the P = O at 1244 cm^{-1}, N−C at 1100 cm^{-1}, and P−O−(C) at 1068, 972 cm^{-1}. The FTIR spectrum of $[P_{4444}][DBP]$ has strong peaks of the P = O at 1234 cm^{-1}, P−O−(C) at 1027, 1002, 983 cm^{-1}, P−O−$[P_{4444}]$ at 810 cm^{-1}, and P−C bonds at 721 cm^{-1}. These NMR and FTIR results confirmed the chemistry of the two ILs.

https://doi.org/10.1021/acssuschemeng.5c03399
ACS Sustainable Chem. Eng. 2025, 13, 12482−12495

Table 1. List of Lubricants Used in the Toxicity, Biodegradability, and Tribological Evaluations

	lubricant	comments
marine toxicity evaluation treat rate: 200 ppm	castrol Optigear Synthetic 800 gear oil (Castrol-220)	baseline lubricant
	PAG (UCON 50-HB-170)	base oil (BT-mix-220 not used because of its solubility in seawater below the target 200 ppm)
	PAG + 5 wt % GA614	base oil + commercial bioderived additive (baseline additive)
	PAG + 5 wt % $[P_{4444}][DBP]$	base oil + candidate IL
	PAG + 5 wt % $[N_{4441}][DBP]$	base oil + candidate IL
biodegradability evaluation	Castrol-220	baseline lubricant
	BT-mix-220 (a blend of BT 22 and BT 75 at a weight ratio of 78.3:21.7)	base oil
	BT-mix-220 + 2 wt % GA614	base oil + baseline additive
	BT-mix-220 + 2 wt % $[P_{4444}][DBP]$	base oil + candidate IL
tribological evaluation	Castrol-220	baseline lubricant, VG 220
	BT-mix-220	base oil, VG 220
	BT-mix-220 + 0.5 wt % GA614	base oil + baseline additive, VG 220
	BT-mix-220 + 0.5 wt % $[P_{4444}][DBP]$	base oil + candidate IL, VG 220
	BT-mix-220 + 0.5 wt % $[N_{4441}][DBP]$	base oil + candidate IL, VG 220

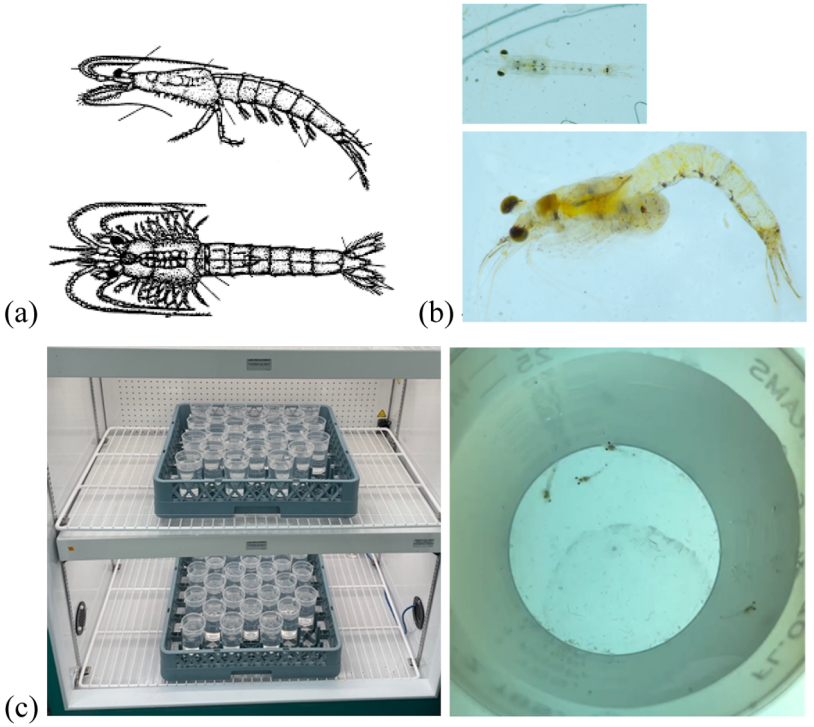

Figure 2. Marine toxicity test. (a) Schematic of a mysid, (b) image of a live juvenile mysid of about 2.2 mm long (top) and a pregnant adult mysid of about 9.0 mm long (bottom), and (c) toxicity test setup.

Thermogravimetric analysis (TGA) was performed on the two ILs using TGA 2950 (TA Instruments) in the air environment and results are displayed in Figure S2 in the Supporting Information. $[P_{4444}][DBP]$ exhibited a lower onset decomposition temperature (175 °C for 10% weight loss) compared with $[N_{4441}][DBP]$ (210 °C).

2.2. Experimental Lubricants. Castrol Optigear Synthetic 800 gear oil with an ISO viscosity grade (VG) of 220 (hereafter represented by Castrol-220) was selected as the baseline lubricant in this work. The measured viscosities at 23, 40, and 100 °C of Castrol-220 are shown in Table S2 in the Supporting Information. Castrol-220 is used in the Siemens gearbox SP240S-MF2 in a model tidal turbine being developed by a joint team of Sandia National Laboratories (SNL), University of New Hampshire (UNH), Pacific Northwest National Laboratory (PNNL), and National Renewable Energy Laboratory (NREL).[40]

One base oil, referred to as BT-mix-220, that is a blend of BT22 and BT75 synthetic esters from Biosynthetic Technologies was used in the tribological and biodegradability tests. Note: The 22 and 75 are not the standard VG numbers but the company's product numbers. The viscosities of BT22 and BT75 are shown in Table S2. Based on the Refutas equation[41] (see a simplified version below), a blend weight ratio of 78.3:21.7 between the BT22 and BT75 was used to produce the BT-mix-220 with a nominal VG 220. The measured viscosities of BT-mix-220 in Table S2 supported that.

$$\nu_{\text{blend}} = \exp(\exp(\chi_{\text{BT22}} \bullet \ln(\ln(\nu_{\text{BT22}} + 0.8)) + \chi_{\text{BT75}} \bullet \ln(\ln(\nu_{\text{BT75}} + 0.8)))) - 0.8$$

where υ is the kinematic viscosity in centistokes, and χ_{BT22} and χ_{BT75} are the mass factions of BT22 and BT75 in the blend, respectively.

Note: BT-mix-220s solubility in the marine water was below the target treat rate (200 ppm), which made it unsuitable for the marine toxicity test. Our earlier freshwater toxicity test used another lower-viscosity BT-mix base oil that had a solubility of 400 ppm in freshwater.[39] Instead, a water-soluble polyalkylene glycol (PAG,

https://doi.org/10.1021/acssuschemeng.5c03399
ACS Sustainable Chem. Eng. 2025, 13, 12482−12495

UCON 50-HB-170, Dow Chemical) was used as the base oil in the marine toxicity test in this work.

A commercial bioderived gear oil EP additive package (GA614, Functional Products, Macedonia, OH) was selected as a baseline additive for a side-by-side comparison with the candidate ILs. The GA614 is composed of olefin sulfide (70−75%), phosphoric acid esters, amine salt (15−17%), alkyl aryl amine (3−4%), and alkylated triazole (5−8%) according to the SDS.

In the marine toxicity evaluation, each additive of the two ILs and GA614 was blended into the PAG at 5 wt %. The 5 wt % concentration was chosen because it is considered as the upper bound of the typical concentration range (0.005−5 wt %) of lubricant additives. If an additive is classified as "Not Toxic" at 5 wt %, it can be reasonably inferred that lower concentrations, like the 0.5 wt % used in the following tribological tests, are also "Not Toxic". Thus, a "Not Toxic" classification at 5 wt % would lead to a logical claim of "Not Toxic" for the entire range of 0.005−5 wt % for that additive. Neat PAG (without additives) and the commercial Castrol-220 gear oil were also tested for comparison.

In the biodegradability evaluation, the test substances included Castrol-220, BT-mix-220, BT-mix-200 + 2 wt % $[P_{4444}][DBP]$, and BT-mix-220 + 2 wt % GA614. The other IL $[N_{4441}][DBP]$ was not tested because of the limited number of channels of CO_2 monitoring. The initial intention was to study the impact of the IL and GA614 at 5 wt % on the BT-mix-220s biodegradation. While the ILs have >5 wt % solubility in the BT-mix-220, the GA614 can only dissolve in the BT-mix-220 up to 2 wt %. For fair comparison, 2 wt % was used as the treat rate for both the ILs and GA614 in the BT-mix-220.

In the tribological evaluation, each additive of the two ILs and GA614 was added into the BT-mix-220 at a 0.5 wt % concentration that was selected based on the typical range of concentrations (0.1−2 wt %) for AW/EP additives and the ILs' proven effectiveness in reducing friction and wear in our earlier sliding tests.[37,39] The neat BT-mix-220 base oil and the fully formulated Castrol-220 gear oil were also tested for comparison.

Table 1 summarizes the experimental lubricants used in the toxicity, biodegradability, and tribological evaluations.

The dynamic viscosities of selected lubricants were measured using a Petrolab MINIVIS II viscometer at 23 °C (room temperature, RT), 40 and 100 °C, as summarized in Table S2. The 0.5 wt % addition of ILs to BT-mix-220 seemed to have little effect on the oil viscosity, which agrees with our previous observations of using ILs oil additives at relatively low concentrations.[30−32]

2.3. Marine Toxicity Evaluation. In our earlier study,[39] the two ILs $[P_{4444}][DBP]$ and $[N_{4441}][DBP]$ had demonstrated much lower toxicity than several commercial bioderived AW additives in freshwater toxicity tests using *Ceriodaphnia dubia*.[42] Their marine toxicity is yet unknown and critical for the tidal energy application. Thus, marine toxicity tests were conducted in the Aquatic Ecology Laboratory at ORNL following an EPA standard chronic marine ecotoxicity test protocol (EPA 833-C-09-001, test method 1007.0)[43] using the standard-recommended model organism *Americamysis bahia* (mysid), as shown in Figure 2. Mysid is an estuarine invertebrate generally found in coastal waters and is known for its high sensitivity to a wide range of toxicants. This EPA standard test is designed to both mimic the natural environment of the organisms and maintain the organisms at sufficient health such that negative impact of chemicals if any can be observed.

The 7-day chronic toxicity test was conducted at 26 ± 1 °C. Each lubricant was blended into laboratory control water (Crystal Sea Marine Mix water, 25 ppt salinity) at a concentration of 200 ppm and then sonicated for 20 min before the test. The light regime for culturing was 16 h light and 8 h dark at 10−20 μE/m2/s (50−100 ft-c.). These conditions are recommended by the EPA method and fall into the range of coastal water environment conditions.

Five mysids (Aquatic BioSystems, Fort Collins, CO) were placed in each polystyrene sample container with ∼150 mL test mixed solution and eight replicates were set up for each lubricant, as shown in Figure 2c. Daily feeding of freshly hatched *Artemia nauplii* were provided at a rate of 225 nauplii per mysid per day and the test solution was refreshed every day.[40] Survival of mysids was monitored daily, and growth and reproduction were quantified at the end of the 7-day exposure for toxicity assessment.

2.4. Biodegradability Evaluation. Biodegradability test was conducted on selected lubricants following the OECD 301B guideline (Ready Biodegradability: CO_2 Evolution Test).[44] As illustrated in Figure 3, experiments were conducted in 250 mL glass jars (see Figure 3b) containing 150 mL of mineral medium each, into which the test substances were added to achieve a target concentration of 15 mg dissolved organic carbon (DOC)/L. The C concentration in the mineral medium was 15 mg/L, as recommended by the OECD method, and was solely derived from the test substances (lubricants here). The mineral medium contained phosphorus and nitrogen sources, including KH_2PO_4, K_2HPO_4, $Na_2HPO_4{\cdot}2H_2O$, and NH_4Cl, to support microbial growth. The ratio of C:N:P was 15:1.3:116. The samples were incubated at 22 °C for 28 days with an inoculum of aquatic microorganisms harvested from a local stream (see Figure 3b) in an incubator with dark or diffuse light according to OECD 301B. It was intended to be kept dark for the incubations to reduce potential photodegradation during the experiment.

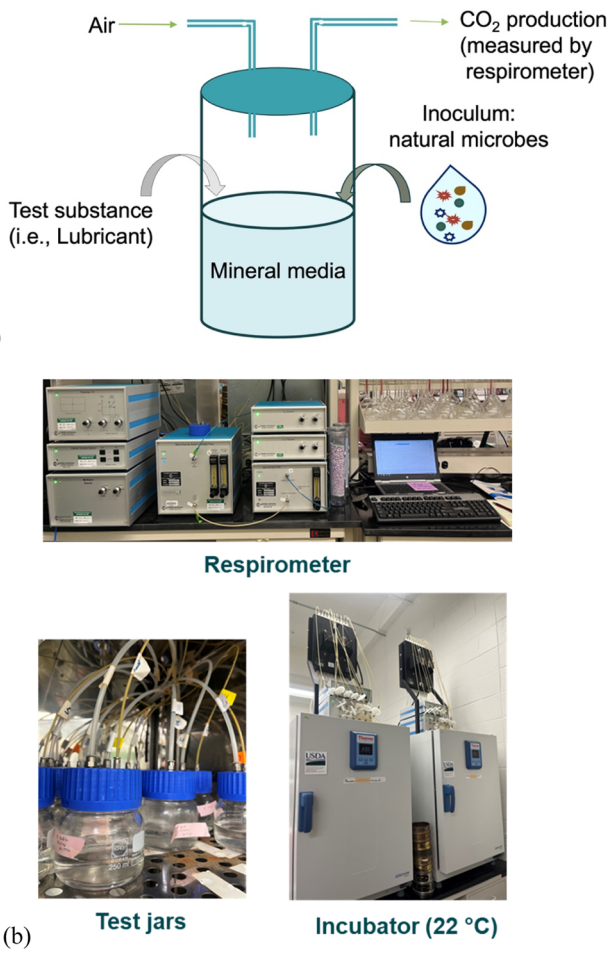

Figure 3. Biodegradability assessment using OECD 301B (respirometry: CO_2 evolution). (a) Schematic and (b) test setup.

Stock solutions of the test substances were prepared in hexane 1 day prior to the experiment to facilitate dissolution in the test medium. The carbon concentration in each stock solution was calculated, and an appropriate volume was added to the mineral medium to reach 15 mg DOC/L. The jars were then shaken with the caps open to allow the hexane to evaporate before incubation. The inoculum was derived from the surface water collected from two locations, upstream and downstream of a wastewater treatment plant, along the East Fork Poplar Creek, East Tennessee. The surface water was filtered through a 0.45 μm membrane and the retained particles were washed with a

https://doi.org/10.1021/acssuschemeng.5c03399
ACS Sustainable Chem. Eng. 2025, 13, 12482−12495

mineral medium. The washout was centrifuged and resuspended in the mineral medium to create a concentrated inoculum.

In each batch, two blanks (inoculum and mineral medium only) and two positive control jars (sodium benzoate, a reference compound recommended by OECD 301B) were included for quality assurance. Test substances were evaluated in two duplicates. The CO_2 production in each jar was monitored using a respirometer (Micro-Oxymax system, Columbus Instruments). The cumulative CO_2 production over a 10-day window (defined as 10 days after 10% of theoretical CO_2 production) was calculated, and the percentage of biodegradation was determined using

$$\text{biodegradation}(\%) = \frac{\text{measured } CO_2 \text{ production}}{\text{theoretical } CO_2 \text{ production}} \bullet 100\%$$

2.5. Tribological Evaluation. The gearbox specifications (Siemens SP240S-MF2-20-0M1/1FT7108-5WC70) and simulated operating conditions of the model tidal turbine were provided by SNL/UNH/PNEL/NREL team to allow us to conduct a tribosystem analysis to determine the critical contact interface of the gearbox and then design a simulative bench-scale tribological test for lubricant evaluation.

According to the literature[45] and our lubrication regime modeling, the front roller bearing of the gearbox was identified as the most vulnerable component to wear and surface damage because of its higher load and lower speed causing a lower oil film thickness. The roller speed of the model turbine was learned to be 30−150 rpm based on the operating simulations by PNNL. The gearbox front bearing shaft surface speed was then determined to be in the range of 0.2−1 m/s with knowing the shaft diameter of 135 mm. The peak contact pressure for the bearing ball against the inner race was simulated in a cycling manner with 2 s at a low load followed by a 1.5-s load ramping up from 0.5 to 1.6 GPa and another 1.5-s load ramping down back to 0.5 GPa (5 s/cycle), according to the literature.[45] It was reported that the operating temperatures of the gearbox bearings in a marine turbine may vary in a range of −30 to 100 °C.[11]

Based on the ranges of speeds, contact pressures, and temperatures determined for the gearbox front bearing of the model tidal turbine as described above, a rolling-sliding test protocol was designed using a micropitting rig (MPR, PCS Instruments) relevant to the contact interface between the bearing's rollers and inner ring. The MPR runs three AISI 52100 bearing steel rings (54 mm dia.) rolling-sliding against an AISI 52100 roller (12 mm dia.) at the center (see Figure 4). All specimens were heat-treated to reach a nominal hardness of HRC 60. The nominal width of the ring-roller contact zone is 1 mm.

The MPR test protocol is shown in Table 2. The mean rolling speed of the MPR roller was a constant 0.19 m/s, near the lower end of the range of 0.2−1 m/s in the actual gearbox front bearing. The sliding-rolling ratio (SRR), where $\text{SRR} = \frac{(v_{\text{roller}} - v_{\text{ring}})}{v_{\text{average of roller and ring}}} \times 100\%$, was set to −2% for the MPR roller. Up to 2% SRR is considered common for roller bearings and the bearing rollers always have negative SRRs relative to the inner ring, because they are driven by the inner ring that is bonded to the rotating shaft.

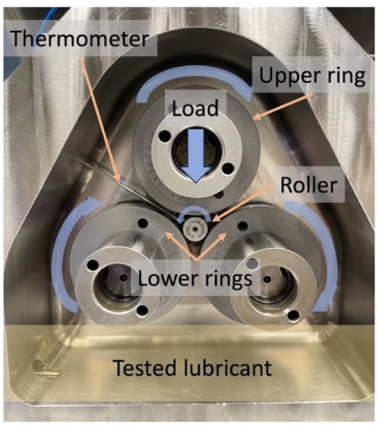

Figure 4. Rolling-sliding tribological test setup using an MPR.

The MPR had difficulties in ramping the load up or down in 1.5 s and thus could not replicate the 5-s loading cycle simulated for the actual gearbox front bearing.[45] Instead, a cycle of 500 s was defined for the MPR test with three stages: (i) 25 N for 200 s to maintain a constant 0.5 GPa Hertzian contact pressure between the roller and rings, (ii) load linearly increasing from 25 to 350 N within 150 s leading to the Hertzian contact pressure gradually rising from 0.5 to 1.6 GPa, and (iii) load linearly dropping back from 350 to 25 N within another 150 s (from 1.6 to 0.5 GPa). The probabilistic S−N curve of JIS SUJ2 bearing steel (equivalent to AISI 52100) in45 suggested contact fatigue surface damage on the bearing rollers after 10^5 stress cycles with an amplitude of 1.6 GPa. Therefore, this test protocol was designed to consist of 40 above-defined load cycles to allow the MPR roller to experience 3.36×10^5 contact cycles.

Two test temperatures, room temperature (RT, about 23 °C in our lab) and 100 °C, were used to simulate the normal and extreme conditions, respectively, as reported in.11

The lambda ratio (λ) at the roller-ring contact area in the MPR test was calculated by dividing the lubricant film thickness (h) by the composite roughness ($\sigma = \sqrt{R_{q,\text{rings}}^2 + R_{q,\text{roller}}^2}$, where R_q is the root-mean-square (RMS) roughness). Lubrication regimes are commonly defined as boundary (BL, $\lambda < 1$), mixed (ML, $1 \le \lambda < 3$), elastohydrodynamic (EHL, $3 \le \lambda < 10$) and hydrodynamic (HL, $\lambda \ge 10$).[46] The calculated lambda ratios in different stages of the MPR test, as shown in Table 2, suggest boundary lubrication during the entire rolling-sliding tests at both temperatures but the much smaller λ ratio at 100 °C is expected to cause more solid−solid asperity collisions at the contact interface and consequently more wear.

At least two replicate tests were conducted for each lubricant under each condition. The friction coefficient and vibration noise are monitored in situ during the test and the wear loss quantification and surface damage examination were executed after the test. The test roller's surface roughness change and volumetric wear loss were quantified using a Wyko NT9100 white light interferometer. The wear volume was calculated as follows:[47]

$$\Delta V = \frac{\pi}{12}[3d_0(w_1^2 - w_0^2) - \tan\theta(w_1 - w_0)^2 \times (w_0 + 2w_1)]$$
$$\tan\theta$$

where d_0 is the initial roller diameter w_0 and w_1 are the width of the cylinder portion on the roller before and after the test, and θ is the cone angle (20° nominal). Measurements were conducted on at least four different locations on the roller and averaged out.

The surface morphology and chemical composition of the roller before and after the MPR tests was examined using field emission scanning electron microscopy (SEM, Hitachi S-4800) and energy dispersive X-ray spectroscopy (EDS) at 5 kV. Selected worn surfaces were also analyzed using a Thermo Scientific K-α X-ray photoelectron spectrometer (XPS). The photoemitted electrons were analyzed with a hemispherical energy analyzer and composition-depth profiles were generated under a 2 kV ion beam energy with a high current setting.

To further analyze the IL-formed tribofilm thickness and composition, a thin cross section was lifted out from the worn roller surface using a gallium-focused ion beam (FIB, Hitachi NB5000). A ~500 nm thick carbon film followed by another ~500 nm thick tungsten coating was deposited on the worn surface prior to the FIB process to preserve the tribofilm. The FIB-lifted thin section was then examined under 200 kV using scanning transmission electron microscopy (STEM, JEOL JEM 2100) equipped with an OXFORD X-MAX Silicon Drift EDS Detector. The EDS data were analyzed using AZtec (version 3.3) software.

3. RESULTS AND DISCUSSION

3.1. Marine Toxicity. Three end points, i.e., survival, growth, and fecundity, of mysids were used to evaluate the toxicity of candidate lubricants. Figure 5a shows the survival of

https://doi.org/10.1021/acssuschemeng.5c03399
ACS Sustainable Chem. Eng. 2025, 13, 12482−12495

Table 2. Rolling-Sliding Test Protocol Relevant to the Gearbox Front Bearing of the Model Tidal Turbine

stage	load (N)	contact pressure (GPa)	U_e (m/s)	SRR	λ ratio @ RT (23 °C)	λ ratio @ 100 °C	duration	no. of cycles on roller
Running-in	25	0.5	0→0.19	0→2%			500 s	
1	25	0.5	0.19	2%	0.88	0.11	200 s	3360
2	25 → 350	0.5 → 1.6	0.19	2%	0.88 → 0.62	0.11→ 0.08	150 s	2521
3	350 → 25	1.6 → 0.5	0.19	2%	0.62 → 0.88	0.08→ 0.11	150 s	2521
			repeat 1−3 (40 cycles)				∼5.7 h	336,080

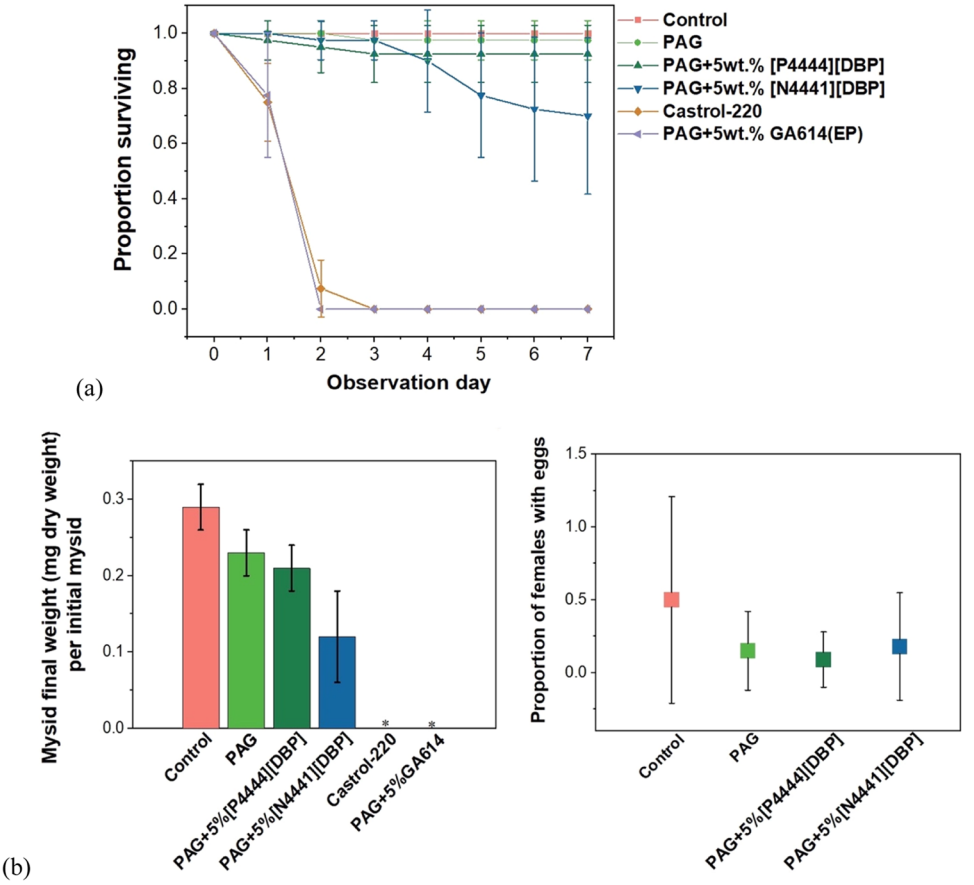

Figure 5. Marine chronic toxicity test results of mysids exposed to experimental lubricants at 200 ppm. (a) Survival of mysids over the 7-day period and (b) growth of mysids measured by weight gain and reproduction measured by proportion of females that had eggs or embryos.

mysids throughout 7 days of exposure to five experimental lubricants at the same 200 ppm concentration. All mysids survived through the 7 days in the control (no exposure to lubricant). It can be clearly seen that all mysids died within 3−4 days in the tests with the commercial baseline, Castrol-220 gear oil, and the lubricant containing the commercial additive, PAG +5 wt % GA 614. In contrast, the mysids exposed to the PAG + 5 wt % IL had more than 90% survival for $[P_{4444}][DBP]$ and ∼70% survival for $[N_{4441}][DBP]$, respectively. Four acute aquatic toxicity categories are defined for the substances by EPA based on 50% survival after 48 h (EC50, crustacea):[48] *Very toxic* for a concentration equal or less 1 mg/L, *Toxic* for a concentration between 1 and 10 mg/L, *Harmful* for a concentration between 10 and 100 mg/L, and *Not toxic* for a concentration higher than 100 mg/L. Therefore, the acute aquatic toxicity of the two ILs, $[P_{4444}][DBP]$ and $[N_{4441}][DBP]$, can be classified as "*Not toxic*" when used at a concentration of 5 wt % or lower, which covers the range of IL concentrations for most applications. As a matter of fact, the tribological test results suggest that even a low 0.5 wt % concentration of these two ILs would provide significant friction and wear reductions, as presented in Section 3.3.

In addition to survival, the growth and fecundity of mysids were also studied. As shown in Figure 5b, both the growth and reproduction of mysids were hindered to some extent when exposed to the neat PAG or PAG-IL blends, in comparison with the control. Note the absence of growth and fecundity data for the commercial gear oil or additive because these end points are measured at the end of 7 days of exposure, and these treatments experienced 100% mortality as a result of these exposures.

In summary, the two ILs exhibited significantly lower toxicity than the commercial additive GA614 at the same concentration in a marine environment. The two PAG+5 wt % IL experimental lubricants are significantly less toxic than the commercial gear oil to mysids and can be categorized as 'Not Toxic' based on EPA's standard.

3.2. Biodegradability. Figure 6 presents the lubricant decomposition percentages as calculated by comparing the CO_2 production over the 10-d window to the theoretical CO_2 production (the concentration of CO_2 that would be expected

https://doi.org/10.1021/acssuschemeng.5c03399
ACS Sustainable Chem. Eng. 2025, 13, 12482−12495

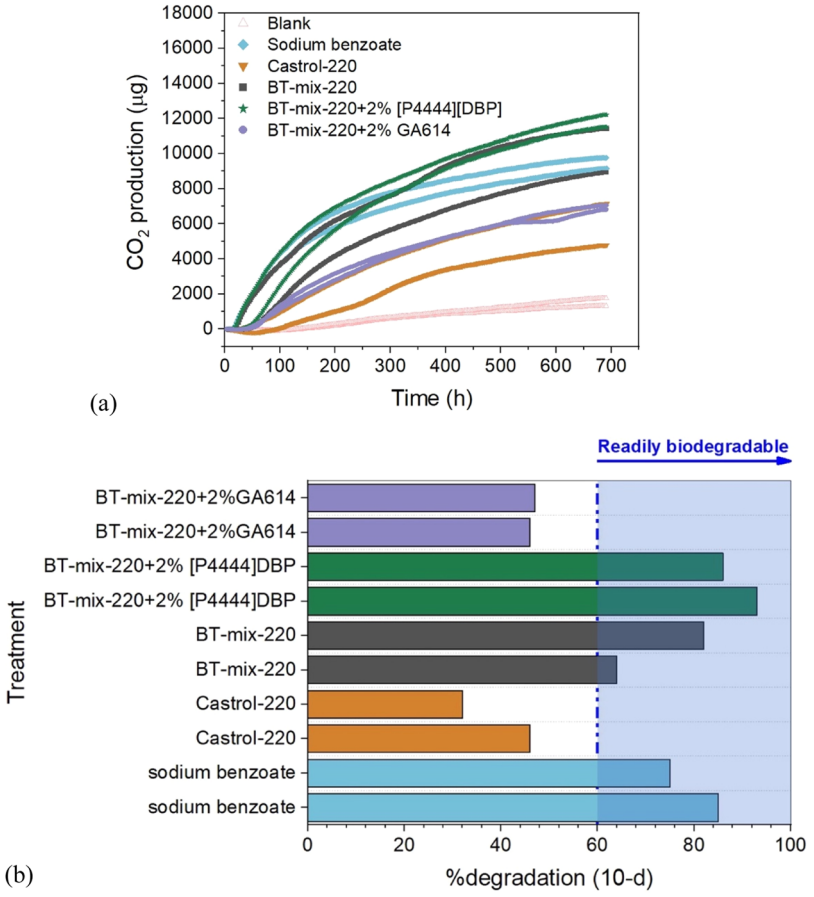

Figure 6. Biodegradation test results of selected lubricants. (a) CO_2 production as a function of time over 28 days and (b) degradation of substances within a 10-day window. Degradation was calculated by comparing the CO_2 production over the 10-day window to the theoretical CO_2 production. Sodium benzoate served as a reference compound as recommended by OECD301B.

if 100% of the compound degraded and evolved as CO_2). Two repeat tests were carried out for the control and each lubricant. The positive control (sodium benzoate) achieved 75 and 85% degradation in the two tests within the 10-day window, meeting the criteria for ready biodegradability (>60%). The commercial Castrol-220 gear oil had decomposition between 32 and 46% within the 10-day window and thus can be classified as inherent biodegradability.

According to the oil specifications from the vendor, both the BT22 and BT75 base oils are readily biodegradable. Thus, the BT-mix-220 (a mixture of these two: 78.3 wt % BT22 + 21.7 wt % BT75) is expected to be readily biodegradable too. Results confirmed the ready biodegradability for the neat BT-mix-220 with 64% and 82% degradation in the two tests, which is consistent with the supplier-reported values of 79% for BT22 and 76% for BT75.

Adding 2 wt % GA614 to the BT-mix-220 slowed down the oil degradation to around 50%, downgrading the lubricant from readily biodegradable to inherently biodegradable. In contrast, the 2 wt % addition of $[P_{4444}][DBP]$ to the BT-mix-220 not only retained the oil's ready biodegradability but also interestingly accelerated the oil degradation to 86 and 93% during the 10-day period in the two repeat tests, respectively.

An additive could affect the oil biodegradation in three aspects: (i) An additive itself may have poor biodegradability, particularly if it contains persistent elements, as suggested by the "Qualitative Substructure Model".[49] For example, additives with large molecular weights, such as ZDDP, may be less accessible to microbes.[18] However, since the typical concentration of an lubricant additive is 0.005−5 wt %, the potential change in the lubricant's overall degradation percentage by an additive would be relatively small, basically limited by its concentration.[20,50,51] (ii) An additive may interact with the base oil molecules to change the oil biodegradability. In this case, one might suspect the IL($[P_{4444}][DBP]$) to possibly catalyze hydrolysis[52] of the BT-mix-220 to split the ester into smaller molecules that might be easier to be accessed and decomposed by the microbes. However, this could not explain why the commercial GA614 slowed down the ester degradation. (iii) An additive may positively or negatively affect the microbial growth and/or activity in decomposing the ester, whose impact could be significant. Phosphorus sources are known to be possibly utilized by microbes and stimulate microbial activity.[53−55] While the mineral media used in the biodegradability test already contained phosphorus compounds, they all were in inorganic forms. Thus hypothetically, the phosphonium-phosphate IL ($[P_{4444}][DBP]$) might have provided organic phosphorus sources to complementarily support the microbial growth and activity,[54,55] consequently leading to accelerated ester decomposition. In contrast, the GA614 contains 70−75% olefin sulfide, which was reported to be toxic to microbes[56,57] and thus could be responsible for the slowed oil degradation. Further investigation using microbial metabolism experiments or elemental analysis is necessary to verify this hypothesis in the future work.

https://doi.org/10.1021/acssuschemeng.5c03399
ACS Sustainable Chem. Eng. 2025, 13, 12482−12495

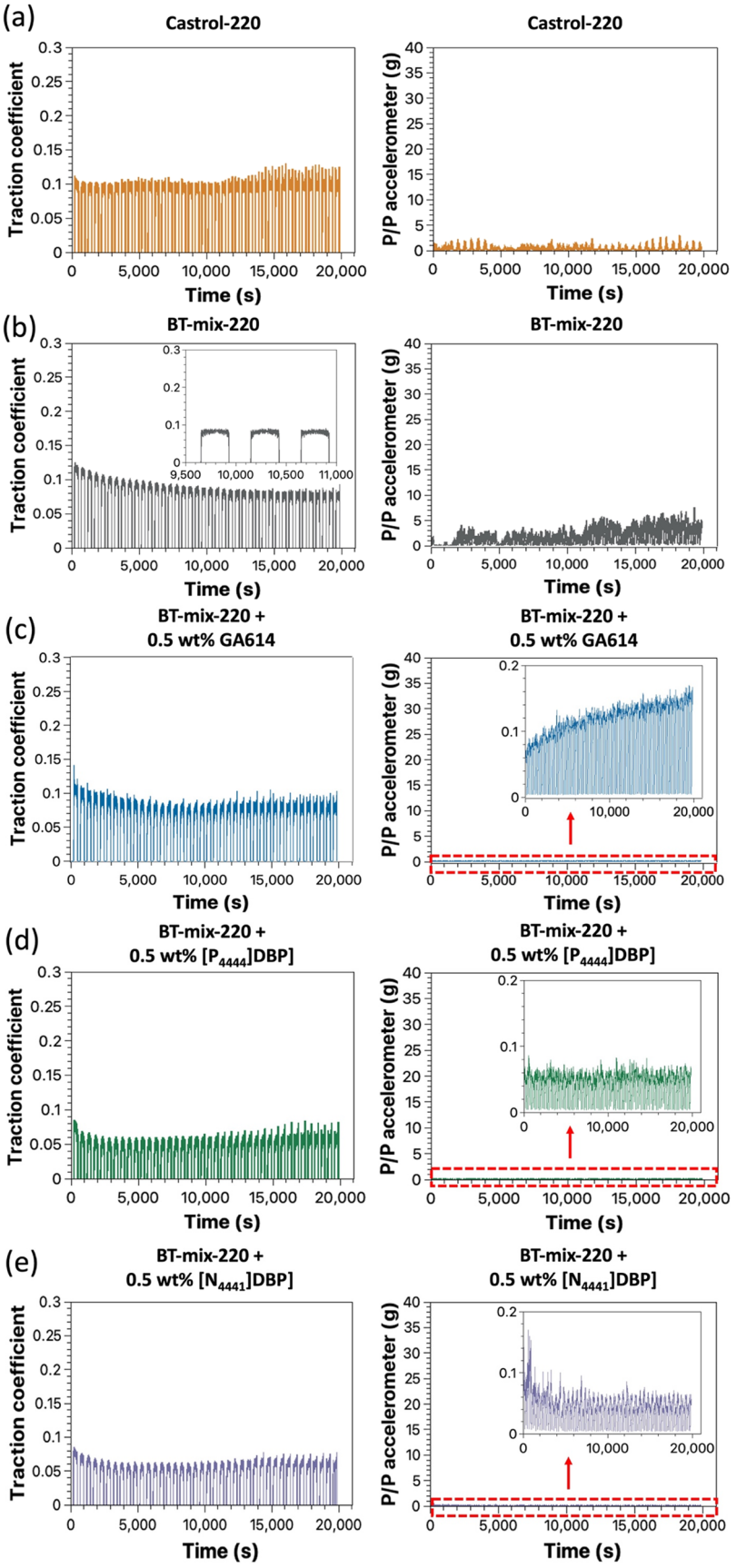

Figure 7. Friction and vibration behavior in the rolling-sliding tests. (a) Castrol-220 gear oil, (b) BT-mix-220 base oil, (c) BT-mix-220 + 0.5 wt % GA614, (d) BT-mix-220 + 0.5 wt % $[P_{4444}][DBP]$, and (e) BT-mix-220 + 0.5 wt % $[N_{4441}][DBP]$. Inserts in (b): zoomed-in friction chart. Inserts in (c–e): zoomed-in vibration charts.

https://doi.org/10.1021/acssuschemeng.5c03399
ACS Sustainable Chem. Eng. 2025, 13, 12482−12495

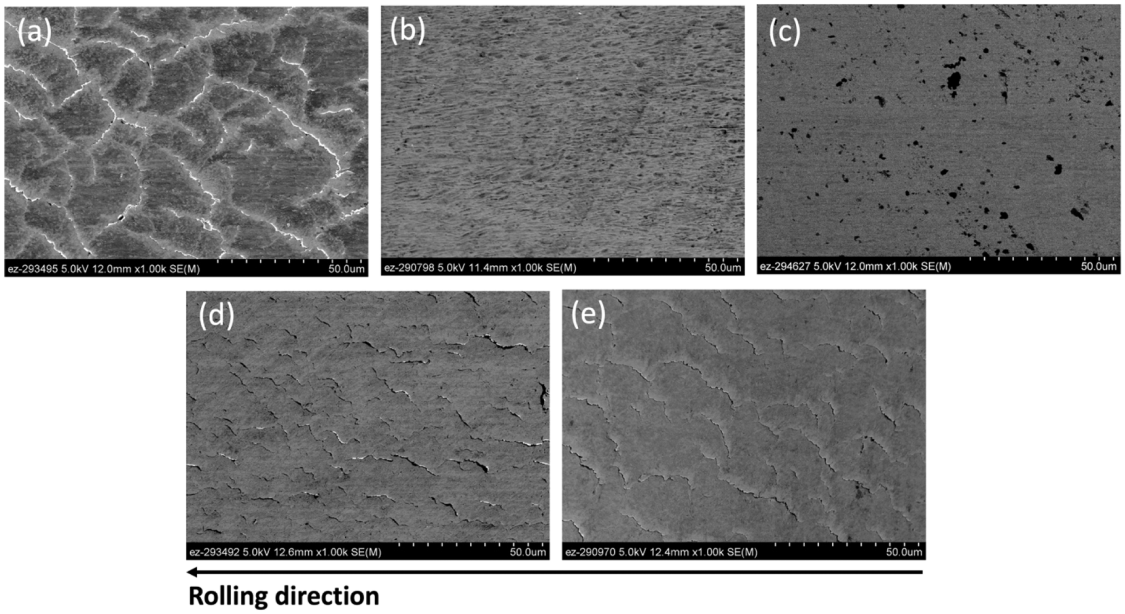

Figure 8. SEM images of the worn roller surfaces from the rolling-sliding tests. (a) Castrol-220, (b) BT-mix-220, (c) BT-mix-220 + 0.5 wt % GA614 and BT-mix-220 + 0.5 wt % ILs including (d) $[P_{4444}][DBP]$, and (e) $[N_{4441}][DBP]$.

3.3. Tribological Behavior. *3.3.1. Lubricating Performance.* Room-temperature rolling-sliding tests were first conducted on three lubricants, i.e., Castrol-220, BT-mix-220 and BT-mix-220 + 0.5% $[P_{4444}][DBP]$ using a designed protocol. No notable distinction in friction, vibration noise, or surface damage was seen among the tests with the three lubricants, as shown in Table S3 and Figures S3 and S4 in the Supporting Information.

Further tribological testing was then carried out using the same protocol but at 100 °C, simulating the extreme operating temperature of the gearbox bearings in a marine turbine.[11] This time, significantly different performance was observed among the five test lubricants, Castrol-220, BT-mix-220, BT-mix-220 + 0.5% GA614, BT-mix-220 + 0.5% $[P_{4444}][DBP]$, and BT-mix-220 + 0.5% $[N_{4441}][DBP]$, as compared in Figures 7 and 8 and Table 3.

Table 3. Wear Volumes and Worn Roller Surface Roughness of Sliding-Rolling Tests at 100 °C

lubricant	wear volume (mm^3)	worn surface roughness R_a (nm)
Castrol-220	0.53 ± 0.02	158 ± 20
BT-mix-220	0.81 ± 0.13	99 ± 10
BT-mix-220 + 0.5 wt % GA614	0.35 ± 0.01	62 ± 33
BT-mix-220 + 0.5 wt % $[P_{4444}][DBP]$	0.29 ± 0.02	137 ± 35
BT-mix-220 + 0.5 wt % $[N_{4441}][DBP]$	0.35 ± 0.03	117 ± 32

The COF of the fully formulated Castrol-220 gear oil remained roughly around 0.1 throughout the test (Figure 7a) and the BT-mix-220 base oil had an initial COF of 0.12 and a steady-state COF of 0.08 (Figure 7b). The 0.5 wt % addition of the commercial GA614 to the BT-mix-220 reduced the initial COF slightly to 0.11 but made little change to the steady-state COF (0.08) (Figure 7c). In contrast, the two ILs showed more effective friction reduction when used as additives in the BT-mix-220 at the same 0.5 wt % concentration (Figure 7d,e). Specifically, the initial COF was reduced to 0.08, which is about 20, 33, and 27% lower compared with the Castrol-220, BT-mix-220, and BT-mix-220 + 0.5% GA614, respectively, and the steady-state COF was reduced to 0.06, which is about 40, 25, and 25% lower than the three baselines, respectively. Because all lubricants here have similar viscosity, the friction reduction by the ILs may be attributed to IL-induced easy-to-shear tribofilms as previously reported for these ILs in pure sliding tests[37,39] and longer-chain ILs in rolling-sliding tests.[32] The tribofilm formed by the $[P_{4444}][DBP]$ in the rolling-sliding test is presented in Section 3.3.2 for validation.

Excellent reduction in vibration noise was also observed for the two ILs. The Castrol-220 had a peak/peak (P/P) acceleration as high as 3 g (Figure 7a). The BT-mix-220s higher P/P acceleration (up to 6 g, Figure 7b) indicated a higher surface damage or wear due to lack of AW/EP additives and was later validated by the wear measurement (Table 3). Adding GA614 to the BT-mix-220 reduced the P/P acceleration by 1 order of magnitude to below 0.2 g (Figure 7c). The two ILs performed even better than the GA614 and reduced the P/P acceleration down to below 0.1 g throughout the test for $[P_{4444}][DBP]$ (Figure 7d) and for most of the time (except a little spike to 0.2 g) for $[N_{4441}][DBP]$ (Figure 7e), respectively.

The wear volumes of the rollers from the rolling-sliding MPR tests are shown in Table 3. The wear loss in the Castrol-220 was 0.53 mm^3 and the wear volume in the BT-mix-220 was higher, 0.81 mm^3, without a surprise because of the lack of AW/EP additives. The three additives, GA614 and two ILs, all demonstrated effective wear protection, reducing to the roller wear loss to 0.35 mm^3 or less. Specially, BT-mix-220 + 0.5 wt % $[P_{4444}][DBP]$ had the lowest wear volume of 0.29 mm^3, which is a 64% reduction compared with the BT-mix-220 base oil and even 45% lower than the fully formulated Castrol-220 gear oil.

The worn roller surfaces are displayed in Figure 8. A network of microcracks induced by RCF were evident on the worn roller lubricated by the Castrol-220 (Figure 8a), and the measured roughness R_a of the worn surface was 158 nm. While the wear loss in the BT-mix-220 was notably higher than that in the

https://doi.org/10.1021/acssuschemeng.5c03399
ACS Sustainable Chem. Eng. 2025, 13, 12482−12495

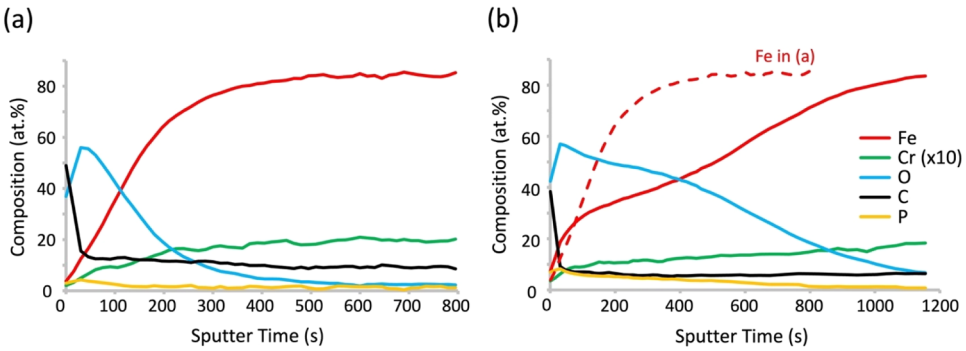

Figure 9. XPS composition-depth profiles of the worn roller surfaces lubricated by (a) BT-mix-220 + 0.5 wt % $[P_{4444}][DBP]$ and (b) BT-mix-220 + 0.5 wt % $[N_{4441}][DBP]$. The dotted line in (b) is the Fe profile copied from (a).

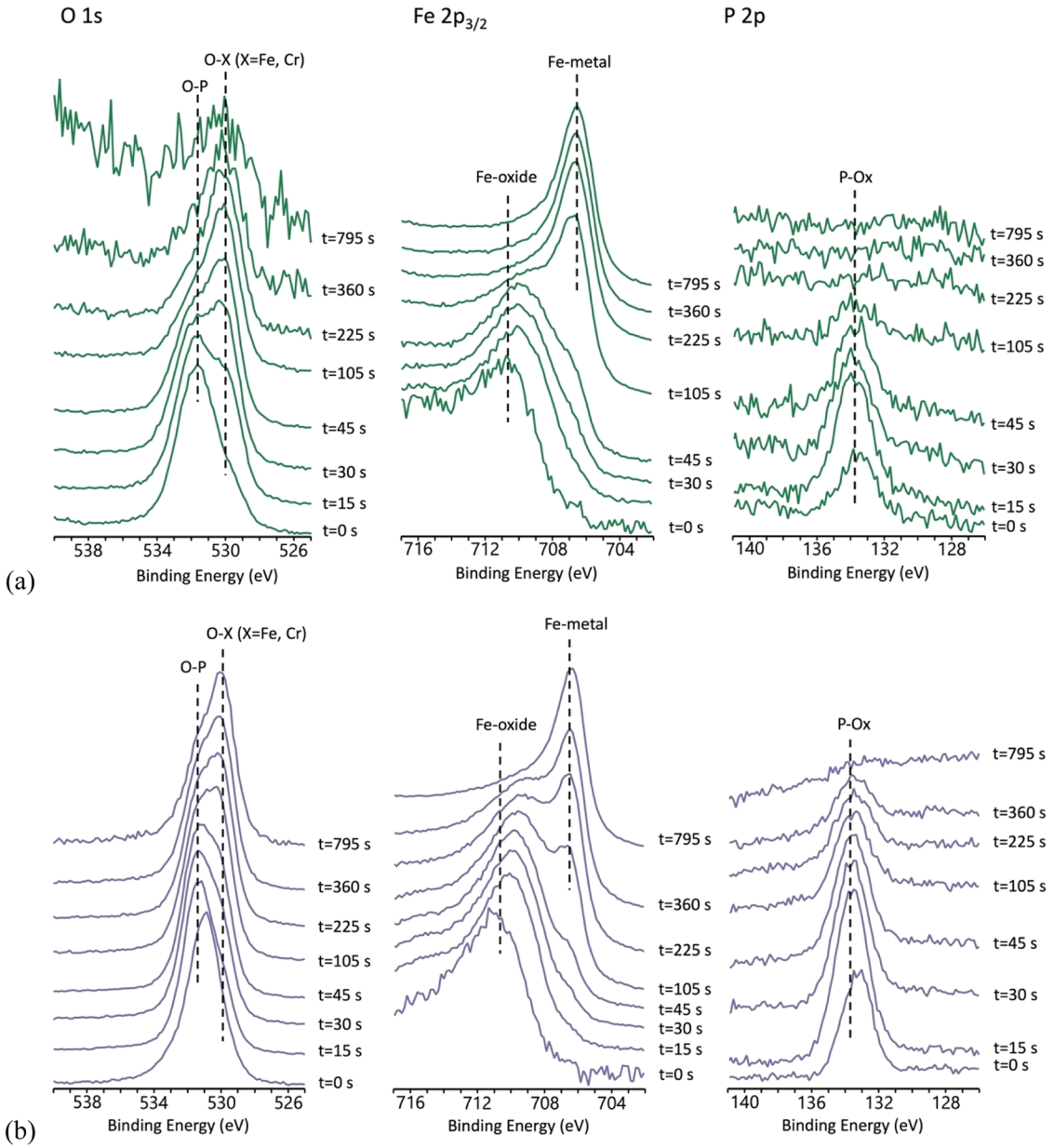

Figure 10. XPS core level spectra at different sputtering depths (0 to 795 s) of O 1s, Fe $2p_{3/2}$ and P 2p for the roller surfaces lubricated by (a) BT-mix-220 + 0.5 wt % $[P_{4444}][DBP]$ and (b) BT-mix-220 + 0.5 wt % $[N_{4441}][DBP]$.

Castrol-220, the worn surface produced by the base oil appears to be smoother (R_a: 99 nm) and cleaner (no visible microcracks, Figure 8b). A rolling-sliding interface always experiences a competition between abrasion and RCF and the worn surface

https://doi.org/10.1021/acssuschemeng.5c03399
ACS Sustainable Chem. Eng. 2025, 13, 12482−12495

morphology reflects the dominating phenomena. When lubricated by the fully formulated Castrol-220, it seems that the AW/EP additives in the gear oil are more effective in protecting the surface from abrasive wear but less effective in mitigating the RCF, and as a result microcracks dominated. In contrast, because the BT-mix-220 does not contain any AW/EP additives, the abrasive wear was significant enough to over-shadow the RCF surface damage (microcracks removed prematurely before growing to visible sizes).

The introduction of the GA614 to the BT-mix-220 provided effective wear protection to the roller (Table 3), but in the meantime the worn surface became even smoother (R_a: 62 nm) and contained numerous small micropits (1−5 μm) whose morphology shares some similarities with corrosion-induced micropits, as shown in Figure 8c. It is hypothesized that the roller surface might have experienced tribocorrosion possibly caused the olefin sulfide (70−75%) in the GA614, which warrants verification in future work.

The two ILs, when added to the BT-mix-220, substantially reduced the abrasive wear (see Table 3 above), which consequently allowed microcracks to grow to some extent, as shown in Figure 8d,8e. Correspondingly, the worn surface roughness increased as well (Table 3). The density and size of the microcracks and roughness are less significant compared with those produced by the Castrol-220 though. There was no sign of tribocorrosion for either IL.

Based on the results above, the two ILs possess superior friction reduction, as effective or even better wear protection, and no tribocorrosion threat compared with the commercial bioderived GA614. Particularly, the BT-mix-220 + 0.5% $[P_{4444}][DBP]$ outperformed the fully formulated Castrol-220 gear oil in terms of reducing friction, wear, and RCF microcracking and thus its tribofilm was selected for detailed characterization as presented below.

3.3.2. Tribofilm Characterization. The above-presented reductions in friction, vibration, wear, and microcracking by the ILs may be attributed to a protective tribofilm generated during the rolling-sliding process, which was observed for these two ILs in pure sliding tests in our earlier work[37,39] as well as longer-chain ILs in rolling-sliding tests in.[32] The tribofilm formation of an IL additive had been proposed as a multistep process starting with direct surface reactions, followed by mechanical deposition through pressing and mixing of wear debris, chemical deposition based on the nucleation of tribochemical reaction products between wear debris and reactive elements, and oxygen diffusion-facilitated oxide interlayer growth.[33]

In this study, XPS analysis from the top surface and STEM examination from the cross-section were used to detect and characterize the tribofilms. Figure 9 presents the XPS composition-depth profiles of the worn rollers tested in the BT-mix-220 + 0.5 wt % $[P_{4444}][DBP]$ and BT-mix-220 + 0.5 wt % $[P_{4444}][DBP]$, respectively. The composition-depth profiles reveal that the primary components on the worn surfaces are C, O, P, and Fe. The concentrations of C, O and P decrease along with the ion sputtering time, following the initial concentration rise during the removal of surface contaminants. The decrease of the O and P contents and the increase of the Fe content appear to be more slowly on the surface lubricated by the BT-mix-220 + 0.5 wt % $[N_{4441}][DBP]$ than that by the BT-mix-220 + 0.5 wt % $[P_{4444}][DBP]$, suggesting that a thicker tribofilm was generated by the $[N_{4441}][DBP]$.

Figure 10 shows the C 1s, O 1s, P 2p and Fe $2p_{3/2}$ core level spectra at different sputtering times for two IL-formed tribofilms. The O 1s peak may be resolved into two peaks, i.e., O−P peak at ∼531.7 eV and metal (e.g., Fe and Cr) oxide peak at ∼530 eV. It suggests that the majority of O atoms are associated with metal oxides and/or iron phosphates. Initially, the tribofilms formed by both ILs seem to contain mainly O−P, likely due to residual IL molecules physically adsorbed on the worn surface. However, during the ion sputtering process, the metal oxide signals, such as O−Fe/P−O-Fe, and metallic Fe peaks gradually grow. The dominant Fe-oxide signal in the $[P_{4444}][DBP]$-formed tribofilm is replaced by the metallic Fe signal after 105 s of sputtering, whereas metallic Fe becomes dominant in the $[N_{4441}][DBP]$-formed tribofilm after 225 s.

In the P 2p spectra, the primary P−O bond (∼133.8 eV) related to phosphates was detected in the tribofilm generated by both ILs. While the P−O signal nearly vanishes in the $[P_{4444}][DBP]$-formed tribofilm after 225 s of sputtering, it remains strong after 360 s. The C 1s spectra, as shown in Figure S5 in the Supporting Information, indicate that the C−C bonding (∼285 eV) dominates in the $[P_{4444}][DBP]$-formed tribofilm within 45 s and in $[N_{4441}][DBP]$-formed tribofilm within 105 s of sputtering.

The XPS chemical analysis validated that the tribofilm induced by $[P_{4444}][DBP]$ is thinner than that formed by $[N_{4441}][DBP]$, and both tribofilms primarily consists of iron oxides and iron phosphates.

To further confirm the existence of the IL-formed tribofilm, a vertical thin section was lifted out of the worn roller surface tested in the BT-mix-220 + 0.5 wt % $[P_{4444}][DBP]$ using FIB. This allowed STEM and EDS to be used to examine the near-surface zone from the cross section, as shown in Figure 11. It can be seen that the $[P_{4444}][DBP]$-formed tribofilm is relatively thin, approximately 10−20 nm and is composed of O, Fe and P, agreeing with the XPS results above.

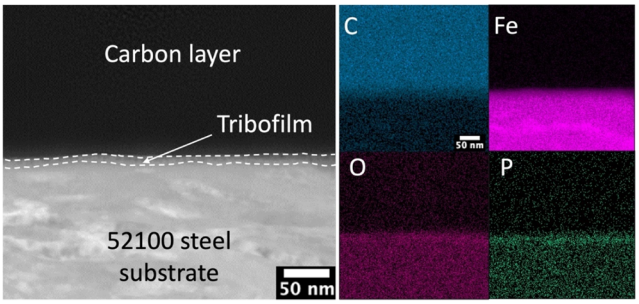

Figure 11. Cross-sectional STEM image of the tribofilm formed on the roller lubricated by BT-mix-220 + 0.5 wt % $[P_{4444}][DBP]$ and corresponding EDS elemental maps. A carbon layer was deposited on the worn surface to prevent the tribofilm from damage during the FIB process.

It is often considered that the IL tribofilm formation is more affected by the anion than by the cation.[58] As shown by the XPS results (Figures 9 and 10), the compositions of both the $[P_{4444}][DBP]$- and $[N_{4441}][DBP]$-formed tribofilm are similar likely due to their identical $[DBP]^-$ anion. On the other hand, the differences in tribofilm thickness (Figures 9 and 10) and surface morphology (Figure 8) suggest that the cation also has impact, agreeing with the literature.[30,59,60] After the initial layer formation, the tribofilm growth is believed to mainly result from a combination of mechanical and chemical deposition[33] and the

https://doi.org/10.1021/acssuschemeng.5c03399
ACS Sustainable Chem. Eng. 2025, 13, 12482−12495

cation could influence the growth rate. The $[N_{4441}]^+$ cation might lead to a more rapid deposition than the $[P_{4444}]^+$ cation, because its smaller size and consequently high mobility would allow more cation−anion pairs to be attracted and moved toward the metal surface to participate in the tribofilm formation. Another point is that the lubricating performance is not necessarily proportional to the tribofilm thickness.[61,62] Here, $[P_{4444}][DBP]$ produced a thinner tribofilm than $[N_{4441}][DBP]$ but it provided a similar friction reduction (Figure 7) and a slightly better wear protection (Table 3). In contrast, it had been observed that the composition[31,63,64] and mechanical properties[31,62] of the tribofilm are more linked to the lubricating behavior.

4. CONCLUSIONS

The marine toxicity, impact on oil biodegradation, and lubricating performance in rolling-sliding of two short-chain ILs, namely $[P_{4444}][DBP]$ and $[N_{4441}][DBP]$, were evaluated as potential EAL additives. An EPA standard aquatic toxicity test demonstrated 70−90% survival of mysids when exposed to 200 ppm of a PAG containing 5 wt % either of the ILs, in contrast to the 0% survival upon exposure of the same concentration of a commercial gear oil or the PAG containing a commercial bioderived additive GA614 at the same 5 wt %. Interestingly, the inclusion of 2 wt % $[P_{4444}][DBP]$ in a synthetic ester not only retained the synthetic ester's ready biodegradability but even increased the decomposition in the 10-day window from a range of 60−80% to a higher level of 80−95%. However, adding 2 wt % of the commercial GA614 reduced the decomposition to below 50%, downgrading the synthetic ester from readily biodegradable to inherently biodegradable. A rolling-sliding test protocol was designed to simulate the critical front bearing of a model tidal turbine gearbox, and demonstrated effective friction reduction, wear protection, and RCF mitigation for the ILs. Addition of the ILs at a 0.5 wt % concentration to the synthetic ester reduced the friction by >50%, wear by >60%, and vibration noise by >95%. The synthetic ester containing 0.5 wt % $[P_{4444}][DBP]$ even outperformed the fully formulated gear oil by ∼40% lower friction coefficient, ∼45% less wear loss, and one order of magnitude lower vibration noise compared with the Castro-220. The IL appeared to be ∼20% more effective in reducing friction and wear than the GA614. Worn surface characterization revealed a protective tribofilm formed by either IL. Morphology and chemical analyses indicated that the anions control the tribofilm composition but the cations affect the film thickness. Results from this fundamental study suggest good feasibility for using ILs as EAL additives and provide a scientific basis for future development. This IL-enhanced EAL technology could benefit tidal energy and broader fields including hydroelectric, hydraulics, water transport, agricultural machinery, offshore wind turbines, etc.

■ ASSOCIATED CONTENT

Supporting Information

The Supporting Information is available free of charge at https://pubs.acs.org/doi/10.1021/acssuschemeng.5c03399.

Lubricant viscosity, proton NMR analysis, FTIR spectra, TGA curves, results of sliding-rolling tests at RT, and additional XPS core level spectra (PDF)

■ AUTHOR INFORMATION

Corresponding Author

Jun Qu − *Materials Science & Technology Division, Oak Ridge National Laboratory, Oak Ridge, Tennessee 37831, United States;* orcid.org/0000-0001-9466-3179; Phone: 865-576-9304; Email: qujn@ornl.gov

Authors

Wenbo Wang − *Materials Science & Technology Division, Oak Ridge National Laboratory, Oak Ridge, Tennessee 37831, United States*

Peijia Ku − *Environmental Sciences Division, Oak Ridge National Laboratory, Oak Ridge, Tennessee 37831, United States;* orcid.org/0000-0003-2813-9269

Louise M. Stevenson − *Environmental Sciences Division, Oak Ridge National Laboratory, Oak Ridge, Tennessee 37831, United States;* orcid.org/0000-0003-4967-9897

Chanaka Kumara − *Materials Science & Technology Division, Oak Ridge National Laboratory, Oak Ridge, Tennessee 37831, United States*

Harry M. Meyer, III − *Chemical Sciences Division, Oak Ridge National Laboratory, Oak Ridge, Tennessee 37831, United States*

Huimin Luo − *Manufacturing Science Division, Oak Ridge National Laboratory, Oak Ridge, Tennessee 37831, United States;* orcid.org/0000-0003-1840-3716

Teresa J. Mathews − *Environmental Sciences Division, Oak Ridge National Laboratory, Oak Ridge, Tennessee 37831, United States;* orcid.org/0000-0001-6780-1142

Complete contact information is available at: https://pubs.acs.org/10.1021/acssuschemeng.5c03399

Author Contributions

This manuscript has been authored by UT-Battelle, LLC, under contract DE-AC05- 00OR22725 with the U.S. Department of Energy (DOE). The U.S. government retains and the publisher, by accepting the article for publication, acknowledges that the U.S. government retains a nonexclusive, paid-up, irrevocable, worldwide license to publish or reproduce the published form of this manuscript, or allow others to do so, for U.S. government purposes. The U.S. DOE will provide public access to these results of federally sponsored research in accordance with the DOE Public Access Plan Access Plan (http://energy.gov/downloads/doe-public-access-plan).

Notes

The authors declare no competing financial interest.

■ ACKNOWLEDGMENTS

The authors thank V. Neary from SNL and R. Cavagnaro from PNNL for providing the design information and operating parameters of the model tidal turbine gearbox, E. Conrad from Syensqo for providing the phosphonium cation feedstock, M. Woodfall, T. Thompson, and J. Holland from Biosynthetic Technologies for supplying the synthetic esters, L. Huffman from Dow Chemical for providing the PAG, and Y.F. Su from ORNL for assistance with the STEM/EDS data acquisition. Research was supported by the Water Power Technologies Office, Office of Energy Efficiency and Renewable Energy, U.S. Department of Energy (DOE).

REFERENCES

(1) Chowdhury, M. S.; Rahman, K. S.; Selvanathan, V.; Nuthammachot, N.; Suklueng, M.; Mostafaeipour, A.; Habib, A.; Akhtaruzzaman, M.; Amin, N.; Techato, K. Current trends and prospects of tidal energy technology. *Environ. Dev. Sustainability* **2021**, *23*, 8179−8194.

(2) Sleiti, A. K. Tidal power technology review with potential applications in Gulf Stream. *Renewable Sustainable Energy Rev.* **2017**, *69*, 435−441.

(3) Kilcher, L.; Fogarty, M.; Lawson, M. *Marine Energy in the United States: An Overview of Opportunities* National Renewable Energy Laboratory: Golden, CO; NREL/TP-5700−78773; 2021 https://www.nrel.gov/docs/fy21osti/78773.pdf.

(4) Touimi, K.; Benbouzid, M.; Tavner, P. Tidal stream turbines: With or without a Gearbox? *Ocean Eng.* **2018**, *170*, 74−88.

(5) Shetty, C.; Priyam, A. A review on tidal energy technologies. *Mater. Today Proc.* **2022**, *56*, 2774−2779.

(6) Neary, V. S.; Lawson, M.; Previsic, M.; Copping, A.; Hallett, K. C.; Labonte, A.; Rieks, J.; Murray, D. *Methodology for Design and Economic Analysis of Marine Energy Conversion (MEC) Technologies, SAND2014−9040*; Sandia National Laboratories: USA, 2014.

(7) Hamrock, B. J.; Dowson, D. *Ball Bearing Lubrication: The Elastohydrodynamics of Elliptical Contacts*; John Wiley & Sons: Hoboken, NJ, 1981.

(8) Chen, L.; Lam, W.-H. A review of survivability and remedial actions of tidal current turbines. *Renewable Sustainable Energy Rev.* **2015**, *43*, 891−900.

(9) Sheng, S. *Wind Turbine Gearbox Reliability Database, Condition Monitoring, and Operation and Maintenance Research Update*; National Renewable Energy Lab (NREL): Golden, CO, United States, 2016.

(10) Hahn, B.; Durstewitz, M.; Rohrig, K. Reliability of wind turbines. In *Wind Energy: Proceedings of the Euromech Colloquium*; Springer: Berlin Heidelberg, 2007.

(11) Wood, R. J. K.; Bahaj, A. S.; Turnock, S. R.; Wang, L.; Evans, M. Tribological design constraints of marine renewable energy systems. *Philos. Trans. R. Soc., A* **2010**, *368* (1929), 4807−4827.

(12) Li, G.; Zhu, W. A Review on Up-to-Date Gearbox Technologies and Maintenance of Tidal Current Energy Converters. *Energies* **2022**, *15* (23), No. 9236.

(13) Rudnick, L. R. *Lubricant Additives: Chemistry and Applications*; CRC press, 2017.

(14) Zeng, X.; Li, J.; Wu, X.; Ren, T.; Liu, W. The tribological behaviors of hydroxyl-containing dithiocarbamate-triazine derivatives as additives in rapeseed oil. *Tribol. Int.* **2007**, *40* (3), 560−566.

(15) Zeng, X.; Wu, H.; Yi, H.; Ren, T. Tribological behavior of three novel triazine derivatives as additives in rapeseed oil. *Wear* **2007**, *262* (5−6), 718−726.

(16) *Environmentally Acceptable Lubricants, EPA 800-R-11−002*, United States Environmental Protection Agency Office of Wastewater Management, 2011, https://www.regulations.gov/document/EPA-HQ-OAR-2012-0580-0037 (accessed Mar 28, 2025).

(17) Wang, W.; Qu, J. Current and candidate additives for environmentally acceptable lubricants—A review. *Friction* **2025**, *13* (4), No. 9440988.

(18) Oulego, P.; Blanco, D.; Ramos, D.; Viesca, J.; Díaz, M.; Battez, A. H. Environmental properties of phosphonium, imidazolium and ammonium cation-based ionic liquids as potential lubricant additives. *J. Mol. Liq.* **2018**, *272*, 937−947.

(19) Li, W.; Jiang, C.; Chao, M.; Wang, X. Natural garlic oil as a high-performance, environmentally friendly, extreme pressure additive in lubricating oils. *ACS Sustainable Chem. Eng.* **2014**, *2* (4), 798−803.

(20) Karmakar, G.; Ghosh, P. Soybean oil as a biocompatible multifunctional additive for lubricating oil. *ACS Sustainable Chem. Eng.* **2015**, *3* (1), 19−25.

(21) Ghosh, P.; Karmakar, G. Evaluation of sunflower oil as a multifunctional lubricating oil additive. *Int. J. Ind. Chem.* **2014**, *5*, 1−10.

(22) Nyholm, N.; Espallargas, N. Functionalized carbon nanostructures as lubricant additives−A review. *Carbon* **2023**, *201*, 1200−1228.

(23) Zhang, Z. J.; Simionesie, D.; Schaschke, C. Graphite and hybrid nanomaterials as lubricant additives. *Lubricants* **2014**, *2* (2), 44−65.

(24) Nunn, N.; Mahbooba, Z.; Ivanov, M.; Ivanov, D.; Brenner, D.; Shenderova, O. Tribological properties of polyalphaolefin oil modified with nanocarbon additives. *Diamond Relat. Mater.* **2015**, *54*, 97−102.

(25) Madannejad, R.; Shoaie, N.; Jahanpeyma, F.; Darvishi, M. H.; Azimzadeh, M.; Javadi, H. Toxicity of carbon-based nanomaterials: Reviewing recent reports in medical and biological systems. *Chem.-Biol. Interact.* **2019**, *307*, 206−222.

(26) Liu, Y.; Zhao, Y.; Sun, B.; Chen, C. Understanding the toxicity of carbon nanotubes. *Acc. Chem. Res.* **2013**, *46* (3), 702−713.

(27) Qu, J.; Bansal, D. G.; Yu, B.; Howe, J. Y.; Luo, H.; Dai, S.; Li, H.; Blau, P. J.; Bunting, B. G.; Mordukhovich, G.; Smolenski, D. J. Antiwear performance and mechanism of an oil-miscible ionic liquid as a lubricant additive. *ACS Appl. Mater. Interfaces* **2012**, *4* (2), 997−1002.

(28) Yu, B.; Bansal, D. G.; Qu, J.; Sun, X.; Luo, H.; Dai, S.; Blau, P. J.; Bunting, B. G.; Mordukhovich, G.; Smolenski, D. J. Oil-miscible and non-corrosive phosphonium-based ionic liquids as candidate lubricant additives. *Wear* **2012**, *289*, 58−64.

(29) Zhou, Y.; Qu, J. Ionic liquids as lubricant additives: a review. *ACS Appl. Mater. Interfaces* **2017**, *9* (4), 3209−3222.

(30) Barnhill, W. C.; Qu, J.; Luo, H.; Meyer, H. M., III; Ma, C.; Chi, M.; Papke, B. L. Phosphonium-organophosphate ionic liquids as lubricant additives: effects of cation structure on physicochemical and tribological characteristics. *ACS Appl. Mater. Interfaces* **2014**, *6* (24), 22585−22593.

(31) Qu, J.; Barnhill, W. C.; Luo, H.; Meyer, H. M., III; Leonard, D. N.; Landauer, A. K.; Kheireddin, B.; Gao, H.; Papke, B. L.; Dai, S. Synergistic effects between phosphonium-alkylphosphate ionic liquids and zinc dialkyldithiophosphate (ZDDP) as lubricant additives. *Adv. Mater.* **2015**, *27* (32), 4767−4774.

(32) Stump, B. C.; Zhou, Y.; Luo, H.; Leonard, D. N.; Viola, M. B.; Qu, J. New functionality of ionic liquids as lubricant additives: mitigating rolling contact fatigue. *ACS Appl. Mater. Interfaces* **2019**, *11* (33), 30484−30492.

(33) Zhou, Y.; Leonard, D. N.; Guo, W.; Qu, J. Understanding tribofilm formation mechanisms in ionic liquid lubrication. *Sci. Rep.* **2017**, *7* (1), No. 8426.

(34) Zhang, Y.; Cai, T.; Shang, W.; Sun, L.; Liu, D.; Tong, D.; Liu, S. Environmental friendly polyisobutylene-based ionic liquid containing chelated orthoborate as lubricant additive: Synthesis, tribological properties and synergistic interactions with ZDDP in hydrocarbon oils. *Tribol. Int.* **2017**, *115*, 297−306.

(35) Gusain, R.; Gupta, P.; Saran, S.; Khatri, O. P. Halogen-free bis (imidazolium)/bis (ammonium)-di [bis (salicylato) borate] ionic liquids as energy-efficient and environmentally friendly lubricant additives. *ACS Appl. Mater. Interfaces* **2014**, *6* (17), 15318−15328.

(36) Stolte, S.; Steudte, S.; Areitioaurtena, O.; Pagano, F.; Thöming, J.; Stepnowski, P.; Igartua, A. Ionic liquids as lubricants or lubrication additives: An ecotoxicity and biodegradability assessment. *Chemosphere* **2012**, *89* (9), 1135−1141.

(37) He, X.; Luo, H.; Mathews, T. J.; Stevenson, L.; Geeza, T. J.; Kumara, C.; Meyer, H. M., III; Qu, J. Minimizing Toxicity and Optimizing Lubricity of Ionic Liquids for Eco-Friendly Lubrication. *ACS Sustainable Chem. Eng.* **2024**, *12* (11), 4344−4355.

(38) Qu, J.; Luo, H. M.; He, X. Ionic liquids containing quaternary ammonium and phosphonium cations, and their use as environmentally friendly lubricant. US#11,760,766. 2023.

(39) He, X.; Stevenson, L. M.; Kumara, C.; Mathews, T. J.; Luo, H.; Qu, J. Comparison of Eco-Friendly Ionic Liquids and Commercial Bio-Derived Lubricant Additives in Terms of Tribological Performance and Aquatic Toxicity. *Molecules* **2024**, *29* (16), No. 3851.

(40) Neary, V. S.; Wosnik, M.; Bichanich, M. C.; Kim, D.; Cavagnaro, R.; Gunawan, B.; Bharath, A.; Wakefield, K.; Harris, S. E.; Forbush, D.; Streit, R.; Lannamann, K.; Houck, D. R. *Open-Source Tidal Energy Converter (OSTEC) Testbed: Design Basis Report*, SAND−10839, 2024.

(41) Maples, R. E. *Petroleum Refinery Process Economics*; Pennwell Books, 2000.

(42) *Short-term Methods for Estimating the Chronic Toxicity of Effluents and Receiving Waters to Freshwater Organisms*, Fourth ed.; U.S. Environmental Protection Agency (EPA), 2002.
(43) *Short-term Methods for Estimating the Chronic Toxicity of Effluents and Receiving Waters to Marine and Estuarine Organisms*, Thirdth ed.; U.S. Environmental Protection Agency (EPA), 2002.
(44) *Test No. 301: Ready Biodegradability, OECD 301B: CO2 Evolution Test*, OECD Guidelines for the Testing of Chemicals, Section 3, OECD Publishing, https://www.oecd.org/en/publications/1992/07/test-no-301-ready-biodegradability_g1gh2913.html (accessed Mar 28, 2025).
(45) Karikari-Boateng, K. A. Accelerated testing of tidal turbine main bearing in a full scale nacelle test rig; University of Exeter2016.
(46) Hamrock, B. J.; Dowson, D. *Ball Bearing Lubrication: The Elasohydrodynamics of Elliptical Contacts*; Wiley: New York, 1981.
(47) Stump, B. C.; Zhou, Y.; Viola, M. B.; Xu, H.; Parten, R. J.; Qu, J. A rolling-sliding bench test for investigating rear axle lubrication. *Tribol. Int.* **2018**, *121*, 450−459.
(48) *Safer Choice and Design for the Environment (DfE) Standard*; U.S. Environmental Protection Agency (EPA), 2009.
(49) Niemi, G. J.; Veith, G. D.; Regal, R. R.; Vaishnav, D. D. Structural features associated with degradable and persistent chemicals. *Environ. Toxicol. Chem.* **1987**, *6* (7), 515−527.
(50) Karmakar, G.; Ghosh, P. Atom transfer radical polymerization of soybean oil and its evaluation as a biodegradable multifunctional additive in the formulation of eco-friendly lubricant. *ACS Sustainable Chem. Eng.* **2016**, *4* (3), 775−781.
(51) Ghosh, P.; Hoque, M.; Karmakar, G. Terpolymers based on sunflower oil/alkyl acrylate/styrene as sustainable lubricant additive. *Polym. Bull.* **2017**, *74*, 2685−2700.
(52) Choi, J.; Nidetzky, B. Ionic liquid as dual-function catalyst and solvent for efficient synthesis of sucrose fatty acid esters. *Mol. Catal.* **2022**, *526*, No. 112371.
(53) Zheng, L.; Ren, M.; Xie, E.; Ding, A.; Liu, Y.; Deng, S.; Zhang, D. Roles of phosphorus sources in microbial community assembly for the removal of organic matters and ammonia in activated sludge. *Front. Microbiol.* **2019**, *10*, No. 1023.
(54) Ali, W.; Nadeem, M.; Ashiq, W.; Zaeem, M.; Gilani, S. S. M.; Rajabi-Khamseh, S.; Pham, T. H.; Kavanagh, V.; Thomas, R.; Cheema, M. The effects of organic and inorganic phosphorus amendments on the biochemical attributes and active microbial population of agriculture podzols following silage corn cultivation in boreal climate. *Sci. Rep.* **2019**, *9*, No. 17297.
(55) Khan, K. S.; Ali, M. M.; Naveed, M.; Rehmani, M. I. A.; Sha, M. W.; Ali, H. M.; Abdelsalam, N. R.; Ghareeb, R. Y.; Feng, G. Co-application of organic amendments and inorganic P increase maize growth and soil carbon, phosphorus availability in calcareous soil. *Front. Environ. Sci.* **2022**, *10* (10), No. 949371.
(56) Carbonero, F.; Benefiel, A. C.; Alizadeh-Ghamsari, A. H.; Gaskins, H. R. Microbial pathways in colonic sulfur metabolism and links with health and disease. *Front. Physiol.* **2012**, *3* (3), No. 448.
(57) Lubrizol. Olefin Sulfides in Lubricant Additives. https://www.Lubrizol.com/Sustainability/Social/Product-Health-and-Safety/Product-Stewardship/Olefin-Sulfides-in-Lubricant-Additives#:~:text=Environmental%20Effects,Regulatory%20Information (accessed Mar 28, 2025).
(58) Yu, B.; Zhou, F.; Mu, Z.; Liang, Y.; Liu, W. Tribological properties of ultra-thin ionic liquid films on single-crystal silicon wafers with functionalized surfaces. *Tribol. Int.* **2006**, *39* (9), 879−887.
(59) Arora, H.; Cann, P. Lubricant film formation properties of alkyl imidazolium tetrafluoroborate and hexafluorophosphate ionic liquids. *Tribol. Int.* **2010**, *43* (10), 1908−1916.
(60) Rahman, M. H.; Khajeh, A.; Panwar, P.; Patel, M.; Martini, A.; Menezes, P. L. Recent progress on phosphonium-based room temperature ionic liquids: Synthesis, properties, tribological performances and applications. *Tribol. Int.* **2022**, *167*, No. 107331.
(61) González, R.; Viesca, J. L.; Battez, A. H.; Hadfield, M.; Fernández-González, A.; Bartolomé, M. Two phosphonium cation-based ionic liquids as lubricant additive to a polyalphaolefin base oil. *J. Mol. Liq.* **2019**, *293*, No. 111596.
(62) Landauer, A. K.; Barnhill, W. C.; Qu, J. Correlating mechanical properties and anti-wear performance of tribofilms formed by ionic liquids, ZDDP and their combinations. *Wear* **2016**, *354-355*, 78−82.
(63) Zhou, Y.; Weber, J.; Viola, M. B.; Qu, J. Is more always better? Tribofilm evolution and tribological behavior impacted by the concentration of ZDDP, ionic liquid, and ZDDP-Ionic liquid combination. *Wear* **2019**, *432-433*, No. 202951.
(64) Kumara, C.; Meyer, H. M., III; Qu, J. Material-Dependent Antagonistic Effects between Soot and ZDDP. *Adv. Mater. Interfaces* **2020**, *7* (6), No. 1901956.

https://doi.org/10.1021/acssuschemeng.5c03399
ACS Sustainable Chem. Eng. 2025, 13, 12482−12495